Draft version: March 30, 2017

1. Introduction

Proposed sections in the introduction:

1. Exoplanet detection – Dominant detection methods (Transit, RV), basic statistics of exoplanets discovered by Kepler Space Telescope.

2. Planet Formation – MMSN, Core accretion/GI models, Planetesimal Formation, Nice Model.

3. Planet Dynamics – Mean Motion Resonance, (planetesimal and gas) Migration, Stability.

4. Numerical Integration – Hamiltonian Dynamics, integrator types (hybrid, symplectic, high order), coordinate systems (jacobi, heliocentric, whds).

2. Numerical Integration

2.1. Hamiltonian Dynamics

The Hamiltonian $\mathcal{H}$ encodes the kinetic and potential energy for a system of N bodies. In its most basic form, the Hamiltonian is:

$$\mathcal{H} = \sum_{i=0}^{N-1} \frac{\mathbf{p}_i^2}{2m_i} - \sum_{i=0}^{N-1} \sum_{j=i+1}^{N-1} \frac{Gm_i m_j}{|\mathbf{r}_i - \mathbf{r}_j|} \tag{1}$$

where $\mathbf{r}_i$, $\mathbf{p}_i$ and m_i are the position, momentum and mass of body i, respectively. The first term in Equation 1 sums the kinetic energies of the system, while the second term sums the potential energies of the system.

The coordinates ($\mathbf{r}$,$\mathbf{p}$) used in Hamiltonian mechanics are canonical, obeying the

fundamental Poisson bracket relations:

$$\{\mathbf{r}_i, \mathbf{r}_j\} = 0, \qquad \{\mathbf{p}_i, \mathbf{p}_j\} = 0, \qquad \{\mathbf{r}_i, \mathbf{p}_j\} = \delta_{ij} \qquad (2)$$

A primary benefit of the Hamiltonian framework is the ease in evolving a N-body system into the future or past via Hamilton's equations:

$$\frac{d\mathbf{p}}{dt} = -\frac{\partial H}{\partial \mathbf{r}}$$
$$\frac{d\mathbf{r}}{dt} = \frac{\partial H}{\partial \mathbf{p}} \qquad (3)$$

Numerically this is trivial to do, with the accuracy of the result being inversely proportional to the size of the timestep, dt. A second benefit is the inherent "area preserving" or symplectic nature of Hamiltonian systems, where the energy error is bound to a finite value (excluding e.g. roundoff errors which grow with time).

In the context of planetary systems Equation 1 can be modified to make the evolution more efficient. For example, we know that a planet will orbit in a Keplerian fashion around a central star, determined by the planet's orbital parameters and stellar mass. In multi-planet systems gravitational interactions between planets will occur, perturbing planets off their original Keplerian trajectories. As a result, the Hamiltonian can be restructured into a "Keplerian" term, $\mathcal{H}_K$, and "Interaction" term, $\mathcal{H}_I$ according to (Wisdom & Holman 1991):

$$\mathcal{H} = \mathcal{H}_K + \mathcal{H}_I$$

If the planets are well separated these gravitational interactions are small, and numerically the system can be evolved by applying Keplerian and Interaction operators in a "leapfrog" manner:

$$E_{\mathcal{H}}(dt) = E_{\mathcal{H}_K}(dt/4) \cdot E_{\mathcal{H}_I}(dt/2) \cdot E_{\mathcal{H}_K}(dt/4) \qquad (4)$$

where $E_X(Y)$ represents the evolution of the system under X for time Y. Equation 4 is a second order evolution scheme, and is the most popular choice for integrating planetary systems.

2.2. Coordinate Systems

As mentioned above the most efficient way to solve the N-body problem is to split the Hamiltonian into Keplerian and Interaction components. In general, the Keplerian and Interaction Hamiltonians take the following form:

$$\mathcal{H}_K = \sum_{i=1}^{N} \frac{\mathbf{p}_i^2}{2m_i} - \frac{Gm_0m_i}{\mathbf{r}_i}, \qquad \mathcal{H}_I = \sum_{i=1}^{N} \sum_{j=1, j\neq i}^{N} \frac{Gm_im_j}{|\mathbf{r}_i - \mathbf{r}_j|} \tag{5}$$

However, there are numerous ways to perform these splits, with each coordinate system having different strengths and weaknesses. The most popular splittings are are discussed below. In all cases $\mathbf{r}$ and $\mathbf{p}$ represent cartesian position and momenta, respectively, N is the total number of particles, and M is the total mass of the system.

2.2.1. Jacobi

Carl Jacobi worked out a coordinate system in which the planet positions are measured relative to the centre of mass of all bodies interior to it. Since a planet's semi-major axis (and hence position) is dependent upon the mass interior to it by Kepler's 3rd law, the evolution of a particle is affected by all bodies interior to it.

The Jacobi position $\mathbf{r}'$ and momentum $\mathbf{p}'$ are a canonical set and are related to the cartesian position and momentum according to (Murray & Dermott 1999):

$$\mathbf{r}'_i = \mathbf{r}_i - \mathbf{R}_{i-1}, \qquad \mathbf{p}'_i = \frac{\eta_{i-1}}{\eta_i}\mathbf{p}_i - \frac{m_i}{\eta_i}\sum_{j=0}^{i-1}\mathbf{p}_j \tag{6}$$

where $\mathbf{R}_i = \frac{1}{\eta_i}\sum_{j=0}^{i} m_j\mathbf{r}_j$ is the centre of mass of all particles interior to body i and $\eta_i = \sum_{j=0}^{i} m_i$ is the sum of masses interior to body i. For the special case of $i = 0$:

$$\mathbf{r}'_0 = \mathbf{R}_N, \qquad \mathbf{p}'_0 = \sum_{j=0}^{N}\mathbf{p}_j \tag{7}$$

The inverse transformations from Jacobi coordinates to cartesian coordinates can be found in Chapter 9.5 of Murray & Dermott (1999).

The benefit of Jacobi coordinates is that the kinetic terms remain a sum of squares (Plummer 1918), making numerical integration a straightforward process according to Equation 4. In addition, these coordinates solve the Two Body and Restricted Three Body Problems exactly. However, the primary disadvantage is that a clear ordering of bodies must be present. For example, in a planetesimal disk orbits cross frequently, and there is no straightforward and (computationally) cheap way to order these bodies.

2.2.2. Democratic Heliocentric

In this coordinate system, positions $\mathbf{Q}$ and momenta $\mathbf{P}$ form a canonical set with $\mathbf{Q}$ measured relative to the central mass and $\mathbf{P}$ measuring barycentric momenta. These coordinates are related to the cartesian position and momenta according to (Duncan et al. 1998):

$$\mathbf{Q}_i = \mathbf{r}_i - \mathbf{r}_0, \qquad \mathbf{P}_i = \mathbf{p}_i - \frac{m_i}{M} \sum_{j=0}^{N} \mathbf{p}_j \tag{8}$$

For the special case of $i = 0$:

$$\mathbf{Q}_0 = \frac{1}{M} \sum_{j=0}^{N} m_j \mathbf{r}_j, \qquad \mathbf{P}_0 = \sum_{j=0}^{N} \mathbf{p}_j \tag{9}$$

The benefit of Democratic Heliocentric coordinates is that they are easy to understand and do not require the knowledge of other bodies to derive their coordinates (unlike Jacobi coordinates). However, these coordinates do not solve the Two Body Problem or Restricted Three Body Problems exactly. In addition, $\mathcal{H}_K$ cannot be cleanly written as shown in Equation 5 due to several cross terms that arise when substituting $(\mathbf{Q},\mathbf{P})$ for $(\mathbf{r},\mathbf{p})$. However, this problem can be rectified by transferring these cross terms into an

additional "Jump" Hamiltonian:

$$\mathcal{H}_J = \frac{1}{2m_0} \left| \sum_{i=1}^{N} \mathbf{P}_i \right|^2 \tag{10}$$

Therefore, the evolution of $\mathcal{H}$ in Equation 4 must be modified to include an additional evolution operator under the Jump Hamiltonian, $E_{\mathcal{H}_J}$. Note that since $\{\mathcal{H}_J, \mathcal{H}_I\} = 0$, the ordering of $E_{\mathcal{H}_I}$ and $E_{\mathcal{H}_J}$ does not matter.

2.2.3. WHDS

The WHDS is a modification of the Democratic Heliocentric mapping that splits the kinetic energy slightly differently. The canonical coordinates $\mathbf{Q}$ and $\mathbf{P}$ have the same form, but the Keplerian, Interaction and Jump steps are now (Laskar & Robutel 1995; Wisdom 2006; Hernandez & Dehnen 2016):

$$\begin{aligned}
\mathcal{H}_K &= \sum_{i=1}^{N} \frac{\mathbf{P}_i^2}{2\mu_i} - \frac{G(m_0 + m_i)\mu_i}{\mathbf{Q}_i} \\
\mathcal{H}_I &= \sum_{i=1}^{N} \sum_{j=1, j \neq i}^{N} \frac{Gm_i m_j}{|\mathbf{Q}_i - \mathbf{Q}_j|} \\
\mathcal{H}_J &= \sum_{i=1}^{N} \sum_{j=1, j \neq i}^{N} \frac{\mathbf{P}_i \cdot \mathbf{P}_j}{m_0}
\end{aligned} \tag{11}$$

where $\mu \equiv m_i m_0 / (m_0 + m_i)$.

The benefit of these coordinates is that, unlike Democratic Heliocentric coordinates, the Two Body and Restricted Three Body Problems are now solved exactly. In addition, like Democratic Heliocentric coordinates, the coordinates of each particle are independent of all other particles. One price to pay for these benefits is that $\{\mathcal{H}_J, \mathcal{H}_I\} \neq 0$, and in Equation 4 $E_{\mathcal{H}_J}$ must be exactly nestled in between the $E_{\mathcal{H}_K}$ and $E_{\mathcal{H}_I}$ operators. In addition, the standard symplectic correctors of Wisdom (2006) cannot be used in this coordinate system, however other correctors may be possible to construct.

2.3. Integrator Types

The three main classes of N-body integrators are symplectic, non-symplectic and hybrid. Symplectic integrators employ a fixed timestep, bounded energy error (excepting roundoff errors which grow with time) and fast integration time. These integrators are best suited for well-separated bodies where $\mathcal{H}_I \ll \mathcal{H}_k$, otherwise the energy error increases dramatically or the timestep must be changed, both of which break symplecticity. The most popular symplectic integrator is the Wisdom-Holman mapping (Wisdom & Holman 1991).

Non-symplectic integrators do not require a fixed timestep and do not have a bounded energy error over time. However, these integrators can employ very accurate and precise numerical convergence schemes, for example the Burlish-Stoer or predictor-corrector algorithms (Press et al. 2002). As a result, non-symplectic integrators are typically more accurate but slower than their symplectic counterparts, and can solve most classes of planetary physics problems. A popular non-symplectic integrator is `IAS15` (Rein & Spiegel 2015).

Hybrid integrators typically mix the symplectic and non-symplectic schemes, applying the symplectic scheme on bodies that are distant and non-symplectic scheme on bodies that are close. However, there are hybrid schemes that purely rely on symplectic principles (Duncan et al. 1998). As a result, hybrid integrators are often an optimal balance between speed and accuracy, especially for problems involving close encounters. The most popular hybrid integrator is `Mercury` (Chambers 1999).

3. Planet Dynamics

3.1. Mean Motion Resonance

Mean motion resonance (MMR) occurs when the orbital period of one planet is an integer ratio of another. Like other types of resonances occuring in nature, MMR results in the amplitude growth of various quantities characterizing the system like eccentricity, semi-major axis and the longitude of pericentre (Murray & Dermott 1999). As a result, the presence of MMR can strongly affect the formation, evolution and longterm stability of planetary systems in a diversity of ways. For example, Kirkwood gaps are unstable regions in the asteroid belt carved by MMRs with Jupiter, while Pluto and Neptune are protected from going unstable due to a 3:2 MMR.

For every $p : q$ MMR (where p and q are integers) there are two important resonant angles:

$$\phi_1 = p\lambda_1 - q\lambda_2 + \varpi_1$$
$$\phi_2 = p\lambda_1 - q\lambda_2 + \varpi_2$$

(12)

where λ is the mean longitude and ϖ is the longitude of periapse. For planets in MMR the time variation of one or both of these resonant arguments must be zero. As a result, MMRs can be modelled in terms of a pendulum oscillating about a stable, fixed point. After some algebra it can be shown that a MMR can be modelled as (Murray & Dermott 1999):

$$\ddot{\phi} = -\omega_0^2 \sin\phi$$

(13)

where ω_0 is the amplitude of libration and is dependent upon the orbital parameters of the system (mass, eccentricity, semi-major axis).

The pendulum model facilitates understanding about certain properties of MMR. For energies larger than a critical energy E_{crit}, the pendulum will circulate over all possible

values of ϕ, while for energies smaller than E_{crit} the pendulum will be in MMR and librate about $\phi = 0$. The critical energy, E_{crit}, defines motion on the separatrix, which separates the circulation and libration regimes. In context of a pendulum, this would correspond to the pendulum suspended vertically in the air with an infinite period of libration.

The strength of a given MMR is related to its width, which in turn is related to the order of the resonance ($= p - q$) and the magnitude of p and q (Murray & Dermott 1999). More fundamentally, the strength of a MMR is related to the mass, eccentricity and mean motions of the planets involved (Murray & Dermott 1999). Stronger MMRs are associated with lower values of p, q and $p - q$, making the 2:1 and 3:2 MMRs the most probable resonant locations in nature. Figure 1 shows the distribution of period ratios for planets discovered by *Kepler*, along with the locations of first and second order MMRs. As can be seen, statistical excesses of planets exist near the 2:1 and 3:2 MMR (Lissauer et al. 2011; Fabrycky et al. 2014; Steffen & Hwang 2015), supporting the idea that these resonances are most capable of trapping planets.

Planets from these statistical pileups are typically a few percent away from exact period commensurability, and dissipative mechanisms have been proposed to transport these planets from exact MMR. The most popular of these mechanisms are tidal (Lithwick & Wu 2012; Batygin & Morbidelli 2013; Delisle et al. 2014), protoplanetary (Rein 2012; Baruteau & Papaloizou 2013; Goldreich & Schlichting 2014), and planetesimal (Moore et al. 2013; Chatterjee & Ford 2015). The formation implications for each mechanism are different, and no clear consensus has yet emerged.

3.2.   Migration

3.2.1.   Planetesimal-Driven Migration

Planetesimals passing through the Hill sphere of a planet will exchange angular momentum via gravity (Ida et al. 2000; Kirsh et al. 2009). If there is an asymmetry to the number of planetesimals interacting with the planet on its near and far sides, a net force will migrate the planet. However, to guarantee migration, planetesimal orbits must decouple from the planet. A massive enough planet (e.g. Jupiter) will directly eject and decouple planetesimals from the system, however if the planet is smaller (e.g. Neptune) planetesimals must decouple by interacting with a neighbouring planet. In addition, for sustained migration the planet must constantly encounter fresh, dynamically cold planetesimals (Gomes et al. 2004).

Since protoplanetary growth is proportional to orbital frequency (Rafikov 2003), planetesimal disks are most likely to exist in the outer reaches of planetary systems where fewer orbital cycles have occurred. In the Solar System, the primordial Kuiper belt is believed to have once been such a planetesimal disk, causing Neptune to migrate outwards into the Kuiper belt and shepherd planetesimals inwards to Jupiter, which subsequently ejected them from the Solar System (Fernandez & Ip 1984). This idea is well supported by observations of the outer Solar System, which show that Pluto, along with a host of smaller bodies, orbit in stable 3:2 MMRs with Neptune (Malhotra 1993, 1995).

3.2.2.   Gas-Driven migration

Since the discovery of the first hot Jupiter (Mayor & Queloz 1995), gas-driven migration is believed to play an important role in shaping exoplanetary systems (Lin et al.

1996). Whenever a fully-formed planet is embedded in a protoplanetary disk, angular momentum can be exchanged via disk-planet torques (Goldreich & Tremaine 1980). The result of this exchange is planetary migration, and this scenario is believed to be common to all young planetary systems. Gas-driven migration comes in two main flavours – Type I and Type II.

Type I migration occurs when low-mass planets are fully embedded in a protoplanetary disk and do not significantly perturb the disk structure (Armitage 2010). At particular resonant locations, known as "Linblad resonances", density waves are excited due to gravitational interactions between the planet and disk (Goldreich & Tremaine 1979). These density waves exchange angular momentum with the planet, and migration occurs when the inner and outer disk interact asymmetrically with the planet (Goldreich & Tremaine 1979). In general, the direction of Type-I migration tends to be inwards towards the central star (Ward 1997).

Type II migration occurs when high-mass Jovian planets significantly modify the structure of the surrounding protoplanetary disk, opening up a gap. This gap locks the planet in place, coupling the migration of the planet to the evolution of the disk (Lin & Papaloizou 1986). The viscous evolution of the disk causes the planet to slowly migrate inwards, at speeds typically one or two orders of magnitude slower than Type-I migration (Ward 1997).

In comparison to planetesimal migration, gas-driven migration is still not well understood. In particular, standard calculations of gas-driven migration are too quick by 1-2 orders of magnitude (Lin & Papaloizou 1986; Tanaka et al. 2002), causing planets to spiral into their central stars before the protoplanetary disk has dispersed. In contrast to this standard view, recent work (Fung & Chiang 2017) has suggested that planets actually do not migrate that much and tend to be better behaved than originally believed.

A consensus on migration has yet to be established, but it is clear that some form of migration must occur in the universe due to the large number of planets in or near MMR (Lissauer et al. 2011; Fabrycky et al. 2014; Steffen & Hwang 2015).

3.3. Stability

The longterm stability of planetary orbits has been studied for hundreds of years by the likes of Issac Newton, Joseph-Louis Lagrange and Carl Friederich Gauss. However, due to the chaotic and non-integrable nature of planetary systems it has been historically difficult to make progress on N-body problems. The chaos in planetary systems is caused by overlapping resonances (Chirikov 1979; Lecar et al. 2001), resulting in the divergence of near-identical systems on long timescales. However, with the aid of computers the equations of motion governing planetary systems can be brute-force integrated into the future or past, allowing scientists to answer fundamental questions that have plagued humans for hundreds of years. For example, it is now known that the Solar System is marginally stable (Sussman & Wisdom 1988; Laskar 1994; Lecar et al. 2001), with Mercury having a 1% chance of colliding with Venus or the Sun within a couple billion years (Laskar & Gastineau 2009). It is also now well established that most known multi-planet systems are packed to capacity, and adding additional planets into these systems would result in dynamical instabilities (Fang & Margot 2013; Pu & Wu 2015).

Although most planetary systems cannot be analytically solved, constraints on these systems can still be derived using analytical means. For example, Wisdom (1980) and Duncan et al. (1989) showed that for small eccentricities in the Restricted 3-Body Problem (R3BP), chaotic orbits (leading to close encounters, collisions and ejections) will occur when the perturber and particle are separated by $\Delta a \leq 1.3 \mu_p^{2/7} a_p$ (where subscript p indicates the perturber). Also associated with the R3BP is the Jacobi constant, which can

be used to constrain the chaotic motion of a particle in parameter space. For two massive planets, Gladman (1993) showed that orbits are Hill stable if $\Delta a \geq 3.46 R_H$ (where R_H is the mutual Hill radius), forbidding close encounters for all time.

Since the discovery of numerous exoplanetary systems via *Kepler*, longterm stability has become a popular way to constrain orbital parameters (Lissauer et al. 2011; Steffen et al. 2013; Jontof-Hutter et al. 2014; Tamayo et al. 2015). If one assumes that an observed system is stable over billions of years, grids of N-body integrations can be used to find stable regions of parameter space, further narrowing the range of valid solutions originally constrained by observations. Although this brute-force method is certainly useful, it is not without its costs. A 10 billion year integration or the Solar System takes weeks to complete, and due to the chaotic nature of planetary systems hundreds to thousands of realizations must be simulated to acquire statistically rigorous results.
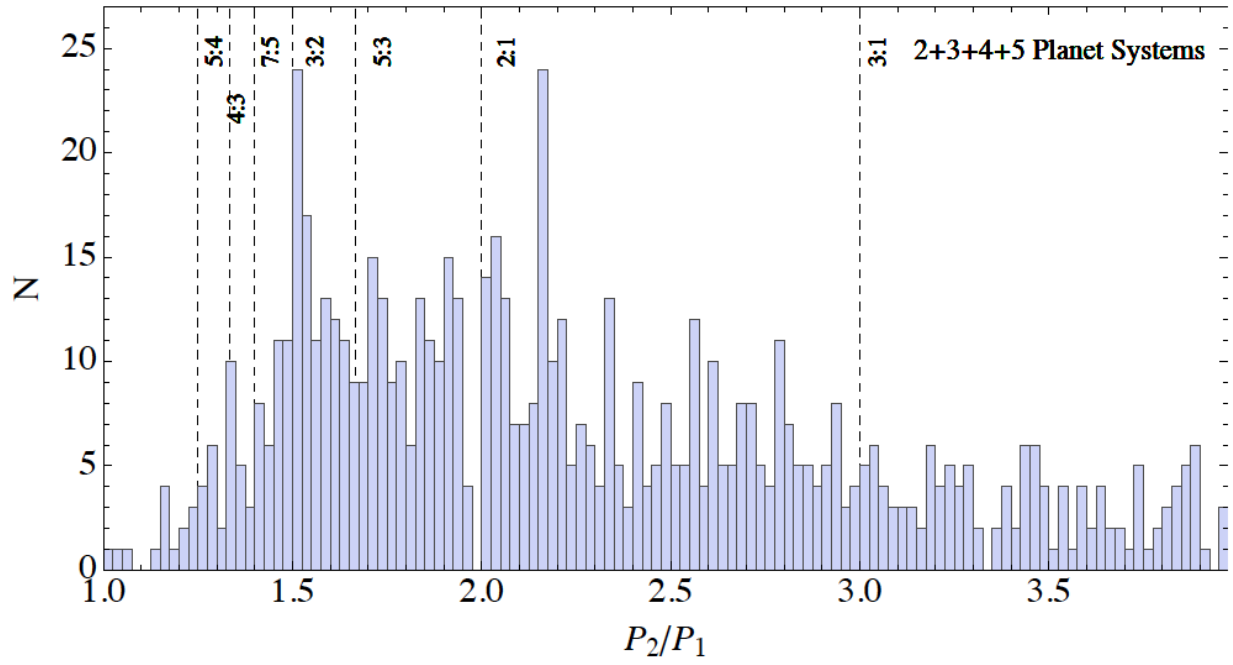
Fig. 1.— Period ratios of Kepler planets, image from Goldreich & Schlichting (2014).

REFERENCES

Armitage, P. J. 2010, Astrophysics of Planet Formation, 294

Baruteau, C., & Papaloizou, J. C. B. 2013, ApJ, 778, 15

Batygin, K., & Morbidelli, A. 2013, AJ, 145, 10

Chambers, J. E. 1999, MNRAS, 304, 793

Chatterjee, S., & Ford, E. B. 2015, ApJ, 803, 10

Chirikov, B. 1979, Physics Review, 52, 263

Delisle, J.-B., Laskar, J., & Correia, A. C. M. 2014, AA, 566, 14

Duncan, M., Quinn, T., & Tremaine, S. 1989, Icarus, 82, 402

Duncan, M. J., Levison, H. F., & Lee, M. H. 1998, AJ, 116, 2067

Fabrycky, D. C., Lissauer, J. J., Ragozzine, D., Rowe, J. F., & Steffen, J. H. 2014, ApJ, 790, 12

Fang, J., & Margot, J.-L. 2013, ApJ, 767, 115

Fernandez, J. A., & Ip, W.-H. 1984, Icarus, 58, 109

Fung, J., & Chiang, E. 2017, ArXiv e-prints, arXiv:1701.08161

Gladman, B. 1993, Icarus, 106, 247

Goldreich, P., & Schlichting, H. E. 2014, AJ, 147, 32

Goldreich, P., & Tremaine, S. 1979, ApJ, 233, 857

—. 1980, ApJ, 241, 425

Gomes, R. S., Morbidelli, A., & Levison, H. F. 2004, Icarus, 170, 492

Hernandez, D. M., & Dehnen, W. 2016, ArXiv e-prints, arXiv:1612.05329

Ida, S., Bryden, G., Lin, D. N. C., & Tanaka, H. 2000, ApJ, 534, 428

Jontof-Hutter, D., Lissauer, J. J., Rowe, J. F., & Fabrycky, D. C. 2014, ApJ, 785, 15

Kirsh, D. R., Duncan, M., Brasser, R., & Levison, H. F. 2009, Icarus, 199, 197

Laskar, J. 1994, A&A, 287, L9

Laskar, J., & Gastineau, M. 2009, Nature, 459, 817

Laskar, J., & Robutel, P. 1995, Celestial Mechanics and Dynamical Astronomy, 62, 193

Lecar, M., Franklin, F. A., Holman, M. J., & Murray, N. J. 2001, ARA&A, 39, 581

Lin, D. N. C., Bodenheimer, P., & Richardson, D. C. 1996, Nature, 380, 606

Lin, D. N. C., & Papaloizou, J. 1986, ApJ, 309, 846

Lissauer, J. J., Ragozzine, D., Fabrycky, D. C., Steffen, J. H., & Ford, E. B. 2011, ApJ, 197, 26

Lithwick, Y., & Wu, Y. 2012, ApJ, 756, 5

Malhotra, R. 1993, Nature, 365, 819

—. 1995, AJ, 110, 420

Mayor, M., & Queloz, D. 1995, Nature, 378, 355

Moore, A., Hasan, I., & Quillen, A. C. 2013, MNRAS, 432, 7

Murray, C. D., & Dermott, S. F. 1999, Solar system dynamics

Plummer, H. C. K. 1918, An introductory treatise on dynamical astronomy

Press, W. H., Teukolsky, S. A., Vetterling, W. T., & Flannery, B. P. 2002, Numerical recipes in C++ : the art of scientific computing

Pu, B., & Wu, Y. 2015, ApJ, 807, 44

Rafikov, R. R. 2003, AJ, 125, 942

Rein, H. 2012, MNRAS, 427, 5

Rein, H., & Spiegel, D. S. 2015, MNRAS, 446, 1424

Steffen, J. H., & Hwang, J. A. 2015, MNRAS, 448, 16

Steffen, J. H., Fabrycky, D. C., Agol, E., et al. 2013, MNRAS, 428, 1077

Sussman, G. J., & Wisdom, J. 1988, Science, 241, 433

Tamayo, D., Triaud, A. H. M. J., Menou, K., & Rein, H. 2015, ApJ, 805, 100

Tanaka, H., Takeuchi, T., & Ward, W. R. 2002, ApJ, 565, 1257

Ward, W. R. 1997, Icarus, 126, 261

Wisdom, J. 1980, AJ, 85, 1122

—. 2006, AJ, 131, 2294

Wisdom, J., & Holman, M. 1991, AJ, 102, 1528